

## Hydrogen-induced surface modifications in ZnO single crystals

This article has been downloaded from IOPscience. Please scroll down to see the full text article.

2011 J. Phys.: Conf. Ser. 262 012050

(<http://iopscience.iop.org/1742-6596/262/1/012050>)

View [the table of contents for this issue](#), or go to the [journal homepage](#) for more

Download details:

IP Address: 86.49.31.183

The article was downloaded on 18/01/2011 at 22:07

Please note that [terms and conditions apply](#).

# Hydrogen-induced surface modifications in ZnO single crystals

I. Prochazka<sup>1</sup>, J Cizek<sup>1</sup>, W Anwand<sup>2</sup>, G Brauer<sup>2</sup>, D Grambole<sup>3</sup> and H Schmidt<sup>3</sup>

<sup>1</sup> Charles University in Prague, Faculty of Mathematics and Physics,  
V Holesovickach 2, CZ-18000 Prague 8, Czech Republic

<sup>2</sup> Institut für Strahlenphysik, Forschungszentrum Dresden-Rossendorf,  
PO Box 510119, D-01314 Germany

<sup>3</sup> Institut für Ionenstrahlphysik und Materialforschung, Forschungszentrum Dresden-Rossendorf, PO Box 510119, D-01314 Germany

E-mail: ivan.prochazka@mff.cuni.cz

**Abstract.** Surface changes in ZnO single crystals electrochemically doped with hydrogen were investigated in this work using slow positron implantation spectroscopy (SPIS) combined with atomic force microscopy (AFM) and optical microscopy. It was found that hexagonally shaped pyramids were formed on the surface of hydrogen-loaded crystals. The formation of these pyramids can be explained by hydrogen-induced plastic deformation realized by a slip in the [0001] direction. Such a picture is supported (i) by AFM where steps of a height comparable with the *c*-lattice parameter were found at the base of the pyramids, and (ii) by SPIS which revealed a defected subsurface layer, formed by the hydrogen-induced plastic deformation and exhibiting an enhanced concentration of open-volume defects in hydrogen-loaded crystals.

## 1. Introduction

ZnO is a wide band gap semiconductor with a variety of applications including UV light emitting diodes, optoelectronic devices, and gas sensors. Due to a progress in crystal growth, high quality single crystals are nowadays available. Properties of ZnO crystals are strongly influenced by lattice defects. A detailed characterization of intrinsic defects and impurities in ZnO crystals is, therefore, very important. Defect studies of hydrothermally grown ZnO single crystals revealed that hydrogen is the most important impurity in ZnO crystals [1]. It was found that hydrogen is coupled with zinc vacancies and vacancy-hydrogen complexes are formed. Moreover, it was shown that a high amount of hydrogen can be introduced into a ZnO crystal by electrochemical loading [2]. In this work, we performed detailed investigations of surface modifications in a hydrogen-loaded ZnO crystal.

## 2. Experimental

A hydrothermally grown ZnO (0001) oriented single crystal (MaTecK GmbH) with O-terminated surface was investigated. The crystal was covered by a 20 nm thick Pd over-layer deposited by cold cathode beam sputtering. The Pd over-layer acts as a catalyst for hydrogen permeation into ZnO and prevents hydrogen losses due to the formation of H<sub>2</sub> molecules on the surface [3]. The specimens were electrochemically doped with hydrogen in a cell filled with an 1:1 mixture of H<sub>3</sub>PO<sub>4</sub> and glycerine. Hydrogen charging was performed at a constant current of 0.3 mA for 24 h using a Pt counter-

electrode and the loaded specimen acting thereby as cathode. The hydrogen concentration introduced into the sample was determined at a depth of  $\sim 100$  nm by nuclear reaction analysis (NRA), employing the resonant nuclear reaction  $^{15}\text{N} + ^1\text{H} \rightarrow ^{12}\text{C} + ^4\text{He} + \gamma$  rays [4] induced by 6.64 MeV  $^{15}\text{N}$  ions. Slow positron implantation spectroscopy (SPIS) investigations were performed on a magnetically guided slow positron beam “SPONSOR” [5]. The energies of incident positrons were selected in the range from 0.03 to 36 keV. Doppler broadened annihilation profiles were analyzed in terms of the S parameters. Atomic force microscopy (AFM) measurements were carried out in the tapping mode using a Dimension DI 3100 microscope (Veeco Instruments). The surface of the specimens was examined also by a metallographic optical microscope (OM) type Arsenal AM-2T.

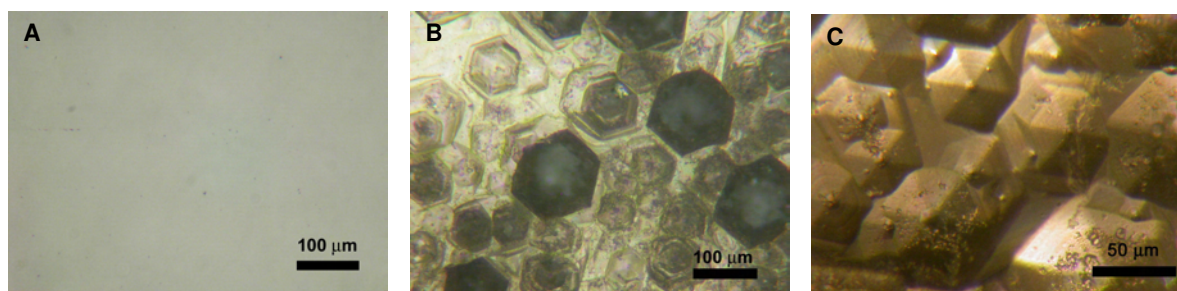


**Figure 1** OM images of ZnO crystal surface. (A) virgin sample (reflected light), (B) hydrogen-loaded sample (loaded side, reflected light), (C) hydrogen-loaded sample (loaded side, glazing incidence light).

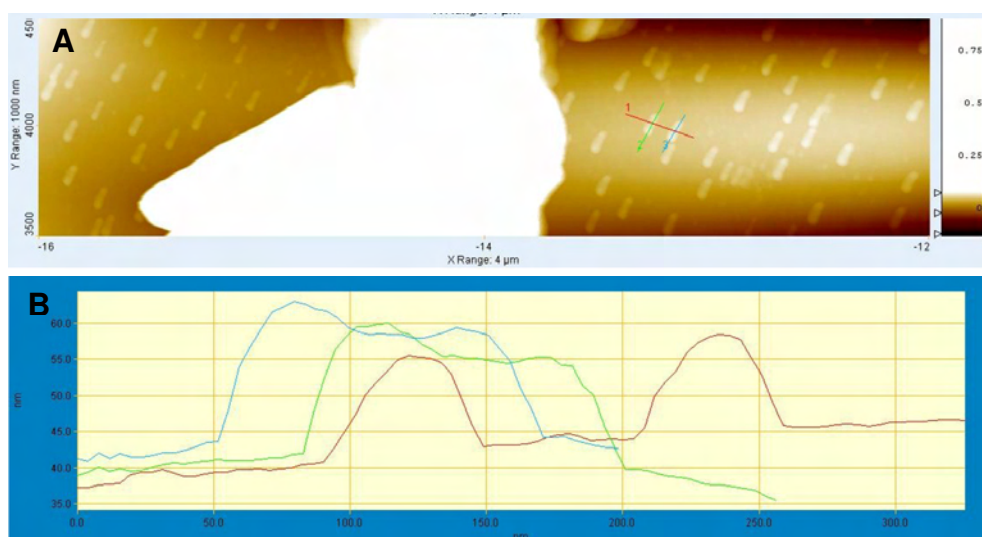


**Figure 2.** (A) AFM image of hydrogen loaded crystal surface showing a lot of crystallites formed by hydrogen loading, (B) height profile taken across the lines 1,2,3 shown in the upper panel.

### 3. Results and discussion

NRA data on the hydrogen-loaded crystal revealed a hydrogen concentration of  $(44.3 \pm 0.1)$  at.-% on the loaded side (covered with Pd cap) and  $(17.2 \pm 0.1)$  at.-% on the backside. These concentrations considerably exceed that of  $(0.3 \pm 0.1)$  at.-% found [1] in the virgin (unloaded) crystal. Hence NRA confirmed a high amount of hydrogen being introduced into the crystal by electrochemical loading. Fig. 1 shows OM images of the sample surface. The virgin crystal exhibits just a flat polished surface (Fig. 1A). However, on the hydrogen-loaded crystal we observed a lot of hexagonal pyramids shown in Fig. 1B. Interestingly, all pyramids have exactly the same orientation with respect to the crystal. Observations in glazing incidence light (Fig. 1C) revealed that the pyramids are grown out of the

sample. The formation of pyramids can be explained by lattice expansion due to hydrogen occupying the bond-centered lattice sites and forming O-H bonds parallel with the  $c$ -axis [6]. When the hydrogen-induced stresses exceed the yield stress, plastic deformation takes place via a slip in [0001] direction.

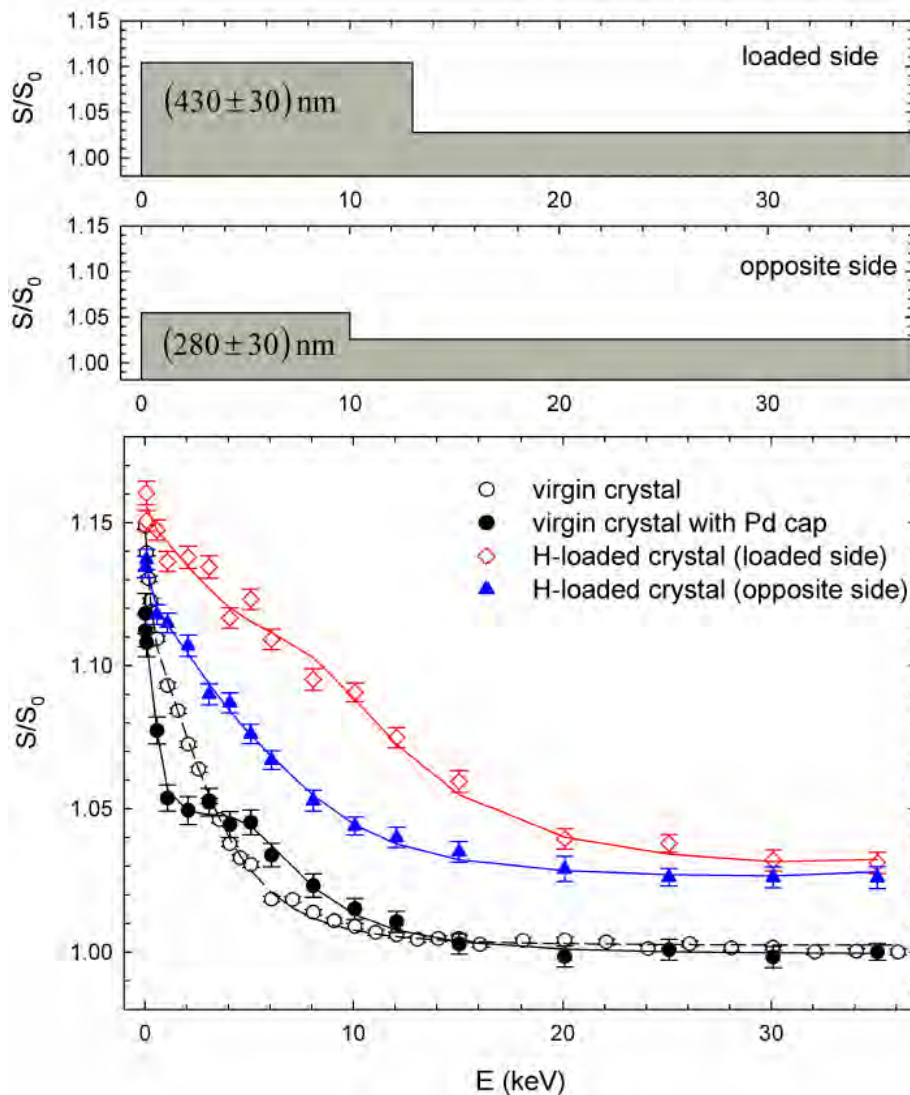


**Figure 3.** Dependence of the S parameter on positron energy  $E$  for the virgin crystal, the virgin crystal covered with Pd cap, and the hydrogen loaded crystal measured on the loaded and the opposite side. All S parameters are normalized to the value  $S_0$  measured on the virgin crystal at  $E = 35$  keV. Solid lines show fit by VEPFIT code [7]. A single layer model was assumed for the virgin crystal. Two layers, including the Pd cap and the ZnO bulk, were used for the virgin crystal covered with the Pd cap. Two layers, involving the defect-rich subsurface layer and the ZnO bulk, were considered for the hydrogen-loaded crystal (the hydrogen-loaded and the opposite side) and are shown in the upper panels. Thicknesses obtained for the defect-rich subsurface layer are given in the upper panels, too.

An AFM image of the hydrogen-loaded crystal is shown in Fig. 2. A lot of tiny crystallites introduced by hydrogen loading can be seen in Fig. 2A. Height profiles of two selected crystallites are plotted in

Fig. 2B. Fig. 2A shows that all nanoscopic bulges have a common orientation with the crystal. Hence AFM testifies that hydrogen loading leads to the formation of nanoscopic features on the surface which may be regarded as nuclei of the micrometer size pyramids observed by OM. This is further supported by the fact that steps with a height comparable to the ZnO *c*-lattice constant were observed by AFM on the slope of these pyramids (Fig. 2B).

SPIS results are plotted in Fig. 3 as dependences of S parameter on positron energy. The solid lines are model curves fitted by the VEPFIT software [7]. Using a single layer model, a relatively short positron diffusion length of  $L_+ = (46 \pm 1)$  nm was determined for the virgin ZnO crystal. Hence, the virgin crystal contains a high density of positron traps. As discussed in detail in Ref. 1 these traps are related to Zn-vacancies. The S(E) curve for the virgin crystal covered with the Pd layer shows a knob around the energy of 2 keV caused by positrons annihilating inside the Pd layer. However, the S parameter for the ZnO bulk is found to remain unchanged. A positron diffusion length of  $L_+ = (47 \pm 2)$  nm obtained by VEPFIT is virtually the same as in the uncovered virgin sample. The S(E) curves measured on the hydrogen loaded crystal (the loaded and the backsides, respectively) are plotted in Fig. 3 as well. One can see from the figure that hydrogen loading leads to a large increase of S parameter in the sub-surface layer corresponding to the positron energy range 1-10 keV and also to an increase of the S parameter for the bulk ZnO region. Hence, two layers involving (i) the sub-surface layer with a very high concentration of defects, and (ii) the bulk ZnO layer were assumed in the VEPFIT analyses of S(E) curves for the loaded crystal. This model is shown schematically in the upper panels in Fig. 3. The formation of a defect-rich sub-surface layer in the hydrogen-loaded crystal strongly supports the picture of hydrogen-induced plastic deformation. Moreover, one can see in Fig. 3 that the S parameter in the defect-rich sub-surface layer is higher on the loaded side of the crystal and the sub-surface layer here also extends more into the bulk of the crystal. An increase of S parameter in the ZnO bulk region indicates that new defects were introduced also into the bulk. However, seemingly the highest concentration of defects was created in the sub-surface layers.

#### 4. Conclusions

A high hydrogen concentration can be introduced into a ZnO crystal by electrochemical loading. Surface studies by OM and AFM revealed the formation of nanometer size bulges in hydrogen-loaded samples which further grow into micrometer size hexagonal pyramids. SPIS investigations revealed an overall increase of the defect density in a hydrogen-loaded crystal and the formation of a defect-rich sub surface layer. These results indicate that structure modifications of hydrogen-loaded samples are likely caused by a slip in [0001] direction caused by stresses arising from a hydrogen-induced lattice expansion.

#### 5. References

- [1] Brauer G, Anwand W, Grambole D, Grenzer J, Skorupa W, Cizek J, Kuriplach J, Prochazka I, Ling C C, So C K, Schulz D and Klimm D 2009 *Phys. Rev. B* **79** 115212
- [2] Cizek J, Zaludova N, Vlach M, Danis S, Kuriplach J, Prochazka I, Brauer G, Anwand W, Grambole D, Skorupa W, Gemma R, Kirchheim R and Pundt A 2008 *J. Appl. Phys.* **103** 053508
- [3] Kirchheim R 1988 *Prog. Mater. Sci.* **32** 261
- [4] Lanford W A 1995 *Handbook of Modern Ion Beam Materials Analysis*, ed R Tesmer and M Nastasi (Pittsburg: Materials Research Society) p 193
- [5] Anwand W, Kissener H-R and Brauer G 1995 *Acta Phys. Polon. A* **88** 7
- [6] Van de Walle C G 2000 *Phys. Rev. Lett.* **85** 1012
- [7] van Veen A, Schut H, Clement M, de Nijs J, Kruseman A and Ijpma M 1995 *Appl. Surf. Sci.* **85** 216

#### Acknowledgments

This work was supported by the Academy of Science of the Czech Republic (project KAN300100801) and the Ministry of Schools, Youths and Sports of the Czech Republic (project MSM 0021620834).